

Gratian Dragoslav Miclaus
Horia Ples

Atlas of CT Angiography



Normal and Pathologic
Findings

 Springer

Gratian Dragoslav Miclaus • Horia Ples

Atlas of CT Angiography

Normal and Pathologic Findings



 Springer

Gratian Dragoslav Miclaus
Department of Computed Tomography
SCM Neuromed
Timisoara
Romania

Horia Ples
Department of Neurosurgery
University of Medicine and Pharmacy
"Victor Babes"
Timisoara
Romania

ISBN 978-3-319-05283-0 ISBN 978-3-319-05284-7 (eBook)
DOI 10.1007/978-3-319-05284-7
Springer Cham Heidelberg New York Dordrecht London

Library of Congress Control Number: 2014942079

© Springer International Publishing Switzerland 2014

This work is subject to copyright. All rights are reserved by the Publisher, whether the whole or part of the material is concerned, specifically the rights of translation, reprinting, reuse of illustrations, recitation, broadcasting, reproduction on microfilms or in any other physical way, and transmission or information storage and retrieval, electronic adaptation, computer software, or by similar or dissimilar methodology now known or hereafter developed. Exempted from this legal reservation are brief excerpts in connection with reviews or scholarly analysis or material supplied specifically for the purpose of being entered and executed on a computer system, for exclusive use by the purchaser of the work. Duplication of this publication or parts thereof is permitted only under the provisions of the Copyright Law of the Publisher's location, in its current version, and permission for use must always be obtained from Springer. Permissions for use may be obtained through RightsLink at the Copyright Clearance Center. Violations are liable to prosecution under the respective Copyright Law.

The use of general descriptive names, registered names, trademarks, service marks, etc. in this publication does not imply, even in the absence of a specific statement, that such names are exempt from the relevant protective laws and regulations and therefore free for general use.

While the advice and information in this book are believed to be true and accurate at the date of publication, neither the authors nor the editors nor the publisher can accept any legal responsibility for any errors or omissions that may be made. The publisher makes no warranty, express or implied, with respect to the material contained herein.

Printed on acid-free paper

Springer is part of Springer Science+Business Media (www.springer.com)

Preface

Permanent research in the field of medical radio-imaging concerning the non-invasive exploration of the circulatory system has led to the appearance and increasing use of the CT multislice for diagnostic purposes.

The acquisition by Neuromed Timisoara of the first computed tomography 64 multislice has placed Romania among the countries using state-of-the-art non-invasive technologies for diagnostic purposes. It is used not only for routine investigations but also in the diagnosis of cardiovascular pathology.

Worldwide the existence and use of this technique avoids almost entirely the use of invasive methods for diagnostic purposes, which takes place only in exceptional circumstances. The invasive part of the diagnosis, which is extremely unpleasant to the patient, is thus eliminated from the diagnostic process, and patients now have the possibility of the diagnosis of vascular pathology without hospitalization.

The technique is also beneficial to the doctors, as it enables them to identify and visualize the exact location of the damaged area, the anatomic details, the severity of lesions leading to a more appropriate planning of the operating techniques by the use of 3D reconstruction.

The present atlas aims to present some of the more challenging cases explored in our clinic during a period of 7 years. During this period, we explored more than 3,500 CT coronary angiographies and more than 18,000 CT angiographies of other anatomic segments.

While the imagistic radiographs presented in this paper do not fully cover the vascular pathology, we consider it useful to present them in the hope that a great number of doctors will become familiar with the exploration possibilities given by this non-invasive method.

The present paper is subject to constant improvement, as our acquired experience and inventory of cases studied, provides us with new and interesting insight to be presented in order to discover more the possibilities of non-invasive exploration of the circulatory system.

Technical Principles

Computed tomography is a diagnostic technique which utilizes X-rays, in which a small fascicle of X-rays axially traverses the patient's body from different angles. Parallel collimation is used to model the fascicle of rays into a small slot, which defines the width of the scanning plan. Detectors measure

the intensity of the reduction of emerging radiation from the patient's body. A mathematical algorithm is used (inverse radon transformation) to calculate the reduction in each part of the CT section. These local reduction coefficients are then transformed into "CT numbers" and are finally converted into shades of grey which are then, in turn, shown as images.

Multislice tomographs allow the acquisition during a single rotation of the tube of a variable number of images (2-6-4), respectively, of a larger volume. The width of the slice is variable, with the spatial resolution growing in reverse proportion with the width. Therefore, for obtaining isotropy, the use of sub-millimetric widths is necessary. Isotopic acquisition allows us to reconstruct images in all three dimensions without modifying the spatial resolution. Thus, diagnostic accuracy in the case of isotopic acquisition is the same, indifferent of the spatial dimension in which the images are later reconstructed.

In the case of Somatom Sensation 64, the spatial resolution of an image is lower than 0.4 mm, and the acquired volume unit (voxel) has the same size for all 3 dimensions (under 0.4 mm for the *x*, *y* and *z* axes).

Obtaining such a resolution is possible due to the technical parameters offered by this machine and, particularly, the high rotation speed of the tube (330 ms) and the technical ability of the STRATON tube to generate two fascicles of X-rays which intertwine, generating the spatial resolution of 0.3 mm.

The length which may be scanned is also important; this machine permits the acquiring of images for a length of up to 1,540 mm, which makes its use possible in peripheral angiographic studies.

All of these technical details, the high scanning speed and high temporal and spatial resolution, allow the use of the computed tomograph in coronary angiographic studies, where the investigation of small arteries belonging to a continually moving organ is necessary.

The study does not aim to become a technical treaty or one of the CT exam protocols, but we consider it necessary to present a couple of technical possibilities for examination as well as a couple of advantages offered by the use of this type of computed tomograph, in relation to the investigated area.

Cerebral CT Angiography

In our clinic, we use a scanning protocol which includes a native scan and a scan which follows the injection of intravenous contrast substance. We apply this protocol in order to obtain the subtraction of the bone, which allows the evaluation of the circulation in the cerebral arteries, without the presence of the bone structures of the neurocranium.

Following the bone subtraction, 3D MIP and 3D VRT reconstructions are used to visualize aneurysms as well as artery-vein malformations (MAV). Coming to the aid of neurosurgeons, we also use 3D VRT reconstructions without bone subtraction, which allows the planning of craniotomies in such a way that the remaining bone defect is at a minimum.

The method is also used to check post-operative evolution in the case of applying metal clips or for selective arterial embolising procedures of the MAV.

CT Angiography of the Cervical Region

This is used to visualize arterial circulation at the level of the cervical region as well as arterial pathology at this level. Thus, we are able to identify stenoses of the common carotid arteries, internal and external; of other arteries at the base of the neck; and of vertebral arteries, as well as perform post-operative or post-interventional checks at the level of the before-mentioned arteries. Thus, one can check the patency of carotid stenting, showing the presence or absence of restenosis in the stent.

Pre-operative details regarding the parietal calcification at the level of the carotid arteries may be given.

As an examination protocol, we use 64×0.6 mm acquisition, with 1 mm reconstruction, and the optimization of the presence of contrast in the carotid arteries is performed through bolus tests.

Post-processing consists of 3D MIP, 3D VRT and 3D MPR reconstructions.

Thoracoabdominal CT Angiography

This is used for visualizing the pathology of the ascending aorta, of the aortic arch and the descending aorta, of the thoracic and abdominal portions and of the branches emerging from these, as well as for studying pulmonary arteries for pulmonary thromboembolism or for malformative pathology.

As a scanning protocol, we use 64×0.6 mm scanning, with a variable rotation of the tube, according to the pathology, with 1 mm reconstructions; in order to find SDC presence in the arterial circulation, we use bolus tests.

Peripheral CT Angiography

This is used for discerning arterial pathology at the level of the lower and upper limbs. It shows the presence of arterial stenoses in obliterating arteriopathy, allows the evaluation of the venous or synthetic graphs used in bypass interventions, as well as the evaluation of the patency of the stents placed at different levels.

It may identify arthero-venous fistulas as well as malformative lesions at the level of the limbs' circulatory bed.

CT Coronary Angiography

CT coronary angiography currently represents one of the most important non-invasive diagnostic possibilities offered by computed tomography.

In our clinic, over the course of 1 year, over 500 patients were investigated with the purpose of detecting coronary affections, as well as patients with stents and aorto-coronary bypasses with the purpose of determining their patency.

In our CT coronary angiography examining protocol, we use native scanning in order to detect and quantify coronary calcifications (Agatston calcium score), followed, if the calcifications are not severe, by the proper angiographic phase. Optimization of the presence of the contrast substance at the coronary level is done through bolus tests, with the quantity of contrast substance administered depending on the scanned surface. In order to reduce the dose administered to the patient, we use CareDOSE 4D and modulated ECG acquisition with pulsed ECG.

The images are acquired in the format 64×0.6 mm, with the reconstruction of axial images at 0.75 mm. Post-processing consists of 3D VRT, 3D MPR and 3D MIP reconstructions. The software of the post-processing unit allows the quantification of the degree of stenosis, expressing the result either as an area or percentage.

Timisoara, Romania

Gratian Dragoslav Miclaus

Contents

1	Cerebral Angiography	1
1.1	Normal Cerebral Angiography	2
1.2	Arteriovenous Malformation at the Level of Pars Precentralis Dextra	4
1.3	Arteria Basilaris Aneurysm at the Level of Pars Proximalis	6
1.4	Arteria Cerebri Media Sinistra Aneurysm	9
1.5	Arteria Cerebri Media Dextra Aneurysm	11
1.6	Aneurysm of Arteria Pericallosa	13
1.7	Aneurysm of Persistent Primitive Hypoglossal Artery	15
1.8	Aneurysm of Arteria Communicans Posterior	17
2	Carotid Angiography	19
2.1	Normal Carotid Angiography	20
2.2	Anomalous Origin of Arteria Carotis Communis	22
2.3	Calcified Atheromatous Plaques at the Level of Arteria Carotis	24
2.4	Carotid Angiography: Nonobstructive Calcified Atheromatous Plaques	26
2.5	Carotid Angiography: Calcified Atheromatous Lesions and Kinking of Arteria Carotis Interna Sinistra	29
2.6	Short Lesion, Moderate Stenosis of Arteria Carotis Interna Sinistra	32
2.7	Carotid Angiography Emphasising a Severe Stenotic Lesion (Subocclusive) at the Level of Arteria Carotis Interna Dextra	35
2.8	Carotid Angiography Emphasising a Subocclusive Lesion at the Level of the Emerging Arteria Carotis Interna Sinistra	38
2.9	Carotid Angiography Ostial Occlusive Lesion at the Level of Arteria Carotis Interna Sinistra	40
2.10	Carotid Angiography: Complete Occlusion of the Arteria Carotis Interna Dextra	43

2.11	Carotid Angiography: Severe Stenotic Lesion at the Level of the Pars Proximalis of Arteria Subclavia Sinistra	45
2.12	Carotid Angiography: Stent Occlusion at the Level of Arteria Subclavia Sinistra	47
3	Thoracic Angiography	49
3.1	Aneurysm of the Aorta Ascendens	50
3.2	Supravalvular Aortic Stenosis	53
3.3	Aneurysm of the Aorta Ascendens: Isthmic Stenosis	56
3.4	Aneurysm of the Arcus Aortae	58
3.5	Aneurysm of the Aorta Ascendens: Chronic Dissection of the Aorta	60
3.6	Post-traumatic Aneurysm of the Aorta Descendens	63
3.7	Gigantic Aneurysm at the Level of the Aorta Descendens	65
3.8	Chronic Dissection of the Aorta Descendens	68
3.9	Stenosis of A. Pulmonalis Dextra	71
3.10	Aneurysm and Dissection of the Aorta ascendens After Valvular Aortic Replacement	73
3.11	Pulmonary Thromboembolism	75
3.12	Right Partially Anomalous Venous Drainage	77
3.13	Partially Aberrant Venous Drainage	79
3.14	Interrupted Arcus Aortae	82
4	Coronary Angiography	85
4.1	Normal Arteriae Coronariae	86
4.2	Abnormal Emergence of the R. Circumflexus	89
4.3	Abnormal Emergence of the A. Coronaria Dextra Placed on the Posterior Aortic Wall	91
4.4	Emergence Through Separate Ostium of the Three A. Coronariae	93
4.5	Abnormal A. Coronaria dextra emergence from the Truncus A. Pulmonalis	95
4.6	Coronary and Aortopulmonary Fistulas	98
4.7	Coronary Calcification	101
4.8	Monovascular Coronary Disease: A. Coronaria Dextra Occlusion	103
4.9	Occlusive Lesion at the Middle Segment of the R. Interventricularis Anterior – Collateral Circulation A. Coronaria Dextra – R. Interventricularis Anterior	105
4.10	Bivascular Coronary Disease	107
4.11	Trivascular Coronary Disease	110
4.12	Aneurysm of the Left Ventricle and R. Interventricularis Anterior Occlusion	113
4.13	Monovascular Coronary Disease Patent Stent in the Middle Segment of R. Interventricularis Anterior	116

4.14	Restenosis at Stent Level	119
4.15	Occlusion of R. Interventricularis Anterior	122
4.16	Coronary Bypass Evaluation.	124
4.17	Fallot Tetralogy	126
4.18	Fallot Tetralogy in an Adult Patient	128
5	Abdominal Angiography	131
5.1	Normal Abdominal Angiography	132
5.2	Aneurysm of Truncus Coeliacus and Stenotic Lesion of A. Hepatica Communis.	135
5.3	Left Renal Arteriovenous Fistula	137
5.4	Aorta Abdominalis Aneurysm with Aortoduodenal Fistula	140
5.5	Operated Aorta Abdominalis Aneurysm: Post-operative Complications.	143
5.6	Stenosis of A. Renalis Sinistra	145
5.7	Right A. Renalis Dextra Occlusion Collateral Circulation for Renal Parenchyma	148
5.8	Dissection of Aorta Abdominalis	151
5.9	Separate Emergence of A. Hepatica Communis and A. Splenica Additional Polar Left Superior A. Renalis Sinistra.	153
5.10	Multiple Aneurysms of A. Splenica Associated with Aneurysm of A. Renalis Dexter	156
6	Peripheral Angiography	159
6.1	Normal Peripheral Angiography	160
6.2	Leriche Syndrome	165
6.3	Leriche Syndrome Axillobifemoral Bypass	167
6.4	Leriche Syndrome Aortobifemoral and Femoropopliteal Graft	170
6.5	Aortobifemoral Graft and Aneurysms at the Level of Anastomosis	174
6.6	Right Arm Occlusion of the Aortobifemoral Graft	177
6.7	Right Femoro-fibular Graft: Occlusion of the Left Lower Limb Arteries.	179
6.8	Iliac and Femoral Stents: In-Stent Restenosis.	182
6.9	Iliac and Femoral Stents: Occluded Iliac Stents	185
6.10	Autoimmune Vasculitis	187
6.11	Tumour of the Leg.	190
6.12	Giant Tumour of the Thigh	192
6.13	CT Angiography of the Right Upper Limb: Occlusion of the Arteria Radialis Dextra	194
6.14	Arteriovenous Malformation in Deltoid Region.	196
6.15	CTA Run-Off: Incidental Finding	198

Contents

1.1	Normal Cerebral Angiography	2
1.2	Arteriovenous Malformation at the Level of Pars Precentralis Dextra....	4
1.3	Arteria Basilaris Aneurysm at the Level of Pars Proximalis	6
1.4	Arteria Cerebri Media Sinistra Aneurysm	9
1.5	Arteria Cerebri Media Dextra Aneurysm	11
1.6	Aneurysm of Arteria Pericallosa	13
1.7	Aneurysm of Persistent Primitive Hypoglossal Artery	15
1.8	Aneurysm of Arteria Communicans Posterior	17

1.1 Normal Cerebral Angiography

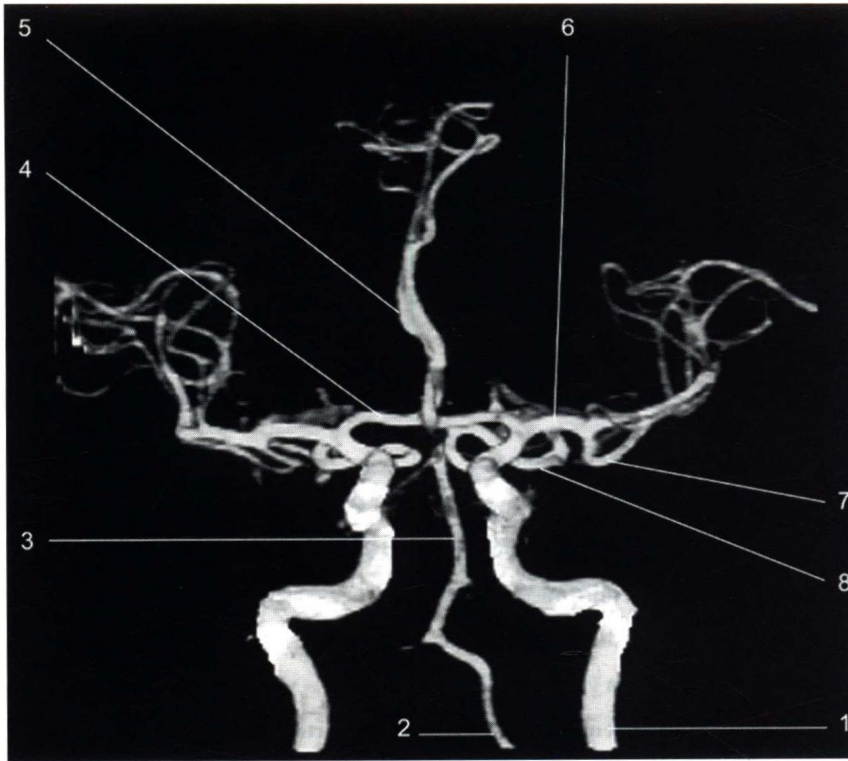


Fig. 1.1 Neuro DSA - VRT

1. A. carotis interna
2. A. vertebralis
3. A. basilaris
4. A. cerebri anterior
5. A. cerebri anterior - segmentum A2
6. A. cerebri media - segmentum M1
7. A. cerebri media - segmentum M2
8. A. cerebri posterior



Fig. 1.2 Neuro DSA - MIP



Fig. 1.3 Neuro DSA - VRT



Fig. 1.4 Neuro DSA – VRT colour



Fig. 1.6 Cerebral angiography 3D VRT reconstruction



Fig. 1.5 Neuro DSA – VRT colour

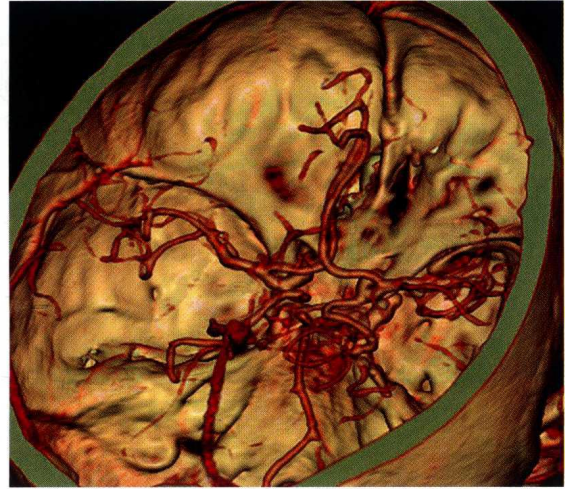


Fig. 1.7 Cerebral angiography 3D VRT reconstruction

1.2 Arteriovenous Malformation at the Level of Pars Precentralis Dextra

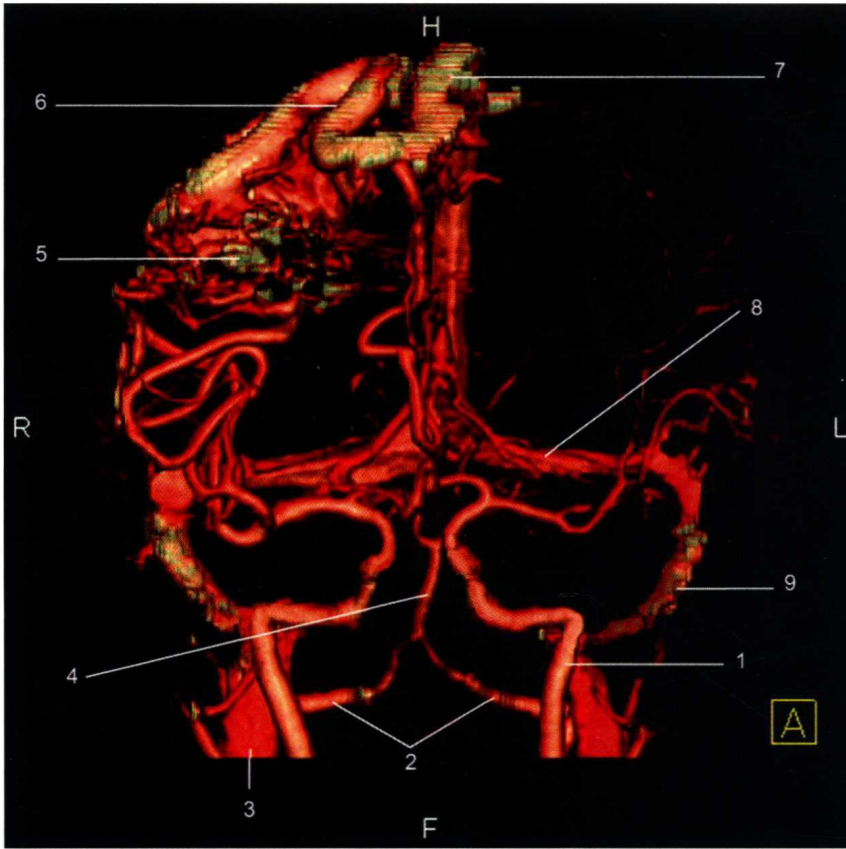


Fig. 1.8 Arteriovenous malformation at the level of pars precentralis dextra
 1. A. carotis interna
 2. A. vertebralis
 3. V. jugularis interna
 4. A. basilaris
 5. Partially embolised arteriovenous malformation
 6. Drainage vein
 7. Sinus sagittalis superior
 8. Sinus transversalis
 9. Sinus sigmoideus

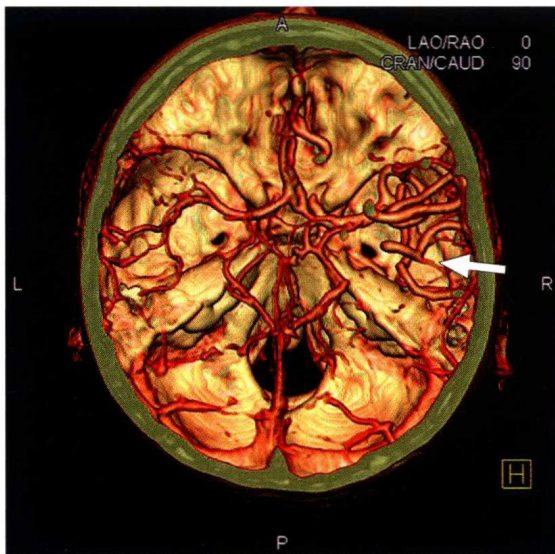


Fig. 1.9 Cerebral angiography in the case of an arteriovenous malformation (*arrow*) (a. cerebra media) with accentuation of the vascularisation at the level of a. cerebra media (3D axial reconstruction)



Fig. 1.10 Cerebral angiography of a partially embolised arteriovenous malformation (*arrow*)

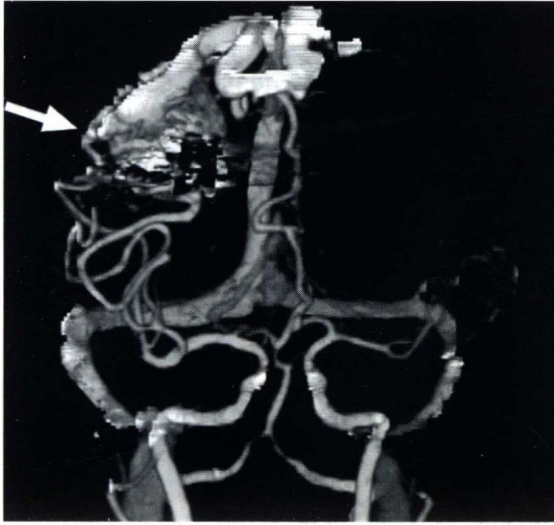


Fig. 1.11 Neuro DSA 3D MIP reconstruction, anterior plan. The *arrow* indicates the arteriovenous malformation

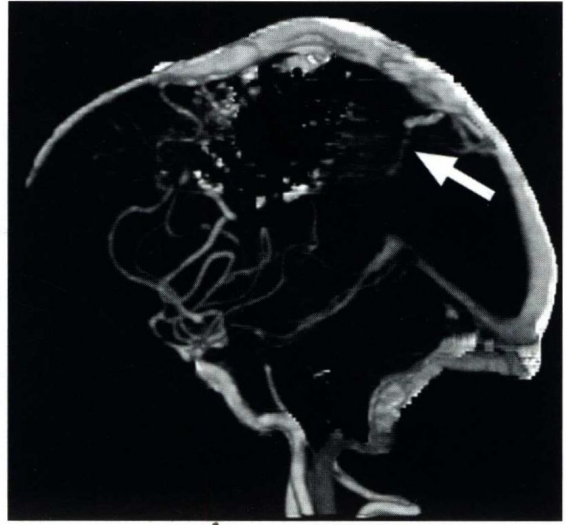


Fig. 1.13 Neuro DSA 3D MIP reconstruction, lateral right plan. The *arrow* indicates the arteriovenous malformation



Fig. 1.12 Neuro DSA 3D MIP reconstruction, posterior view

1.3 Arteria Basilaris Aneurysm at the Level of Pars Proximalis

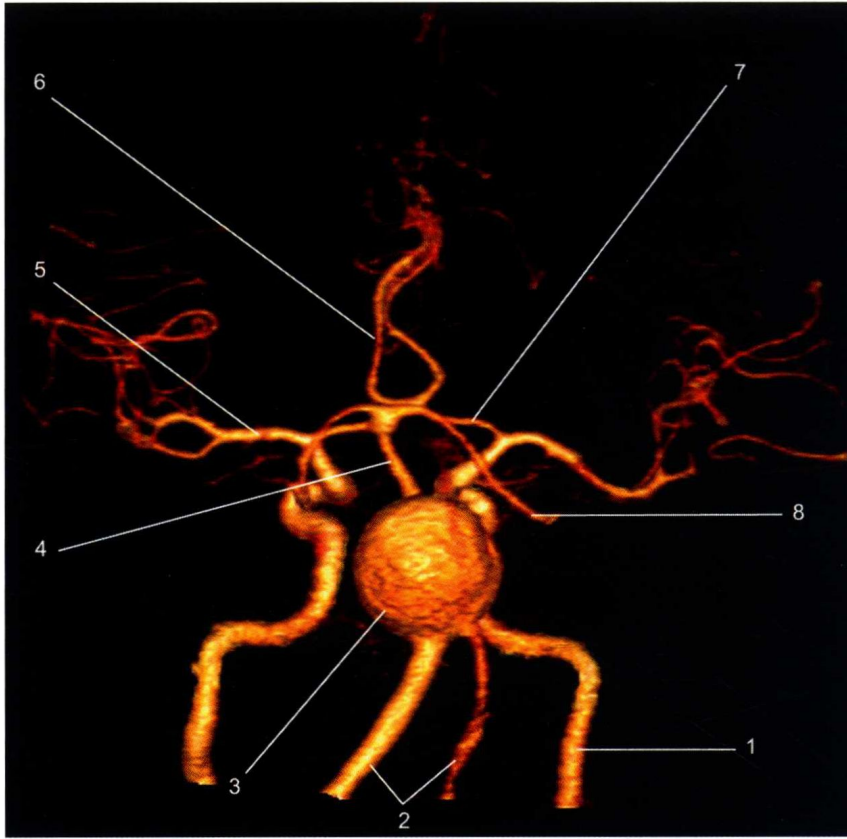


Fig. 1.14 Neuro DSA 3D VRT colour reconstruction

1. A. carotis interna
2. A. vertebralis
3. Giant aneurysm
4. A. basilaris
5. A. cerebri media – segmentum M1
6. A. cerebri anterior – segmentum A2
7. A. cerebri anterior – segmentum A1
8. A. cerebri posterior



Fig. 1.15 Neuro DSA 3D MIP reconstruction

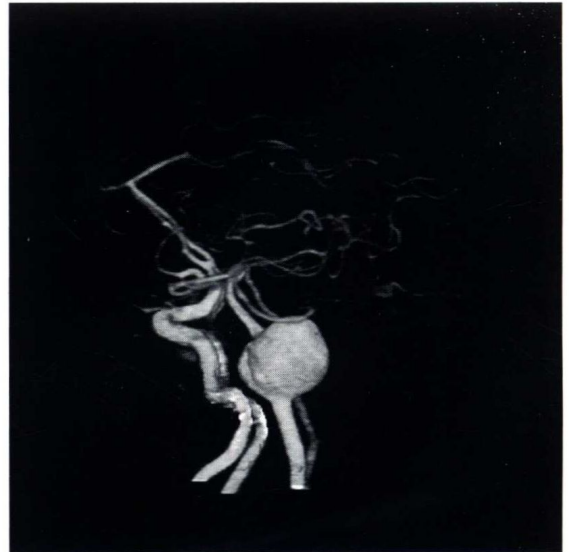


Fig. 1.16 Neuro DSA 3D MIP reconstruction

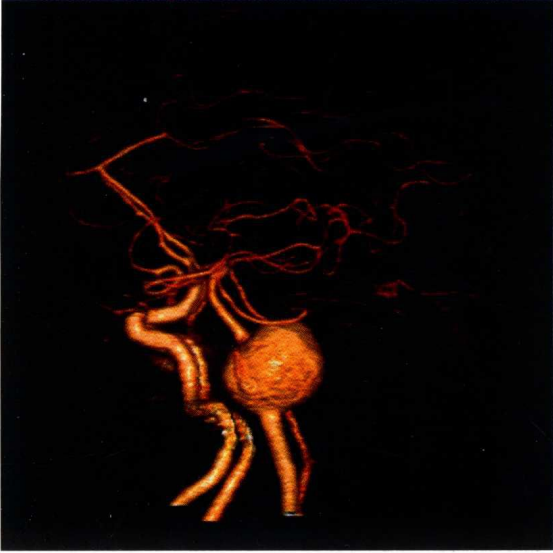


Fig. 1.17 Neuro DSA 3D VRT colour reconstruction

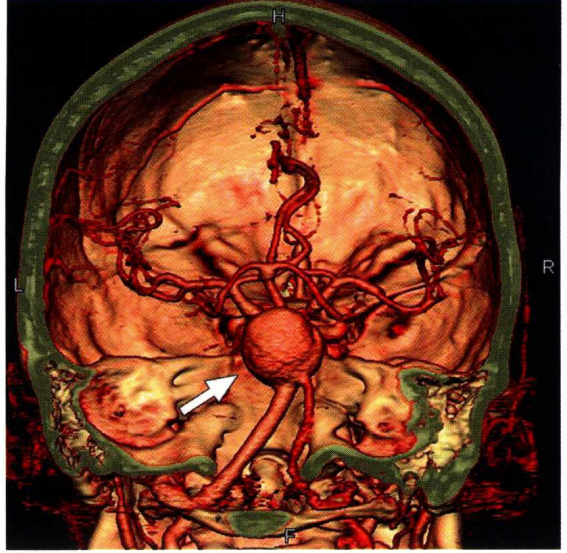


Fig. 1.19 Cerebral angiography 3D VRT reconstruction in posterior coronal plan. The *arrow* indicates the aneurysm

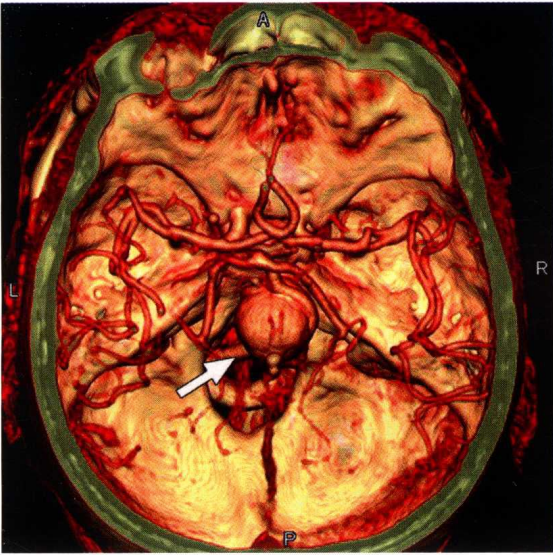


Fig. 1.18 Cerebral angiography axial 3D VRT reconstruction. The *arrow* indicates the aneurysm

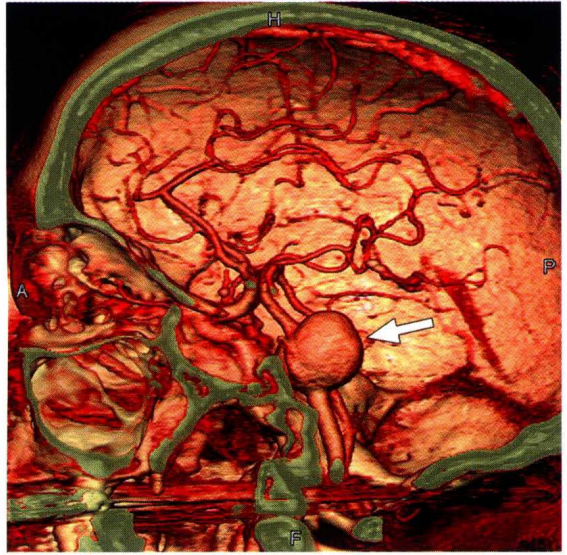


Fig. 1.20 Cerebral angiography 3D VRT reconstruction, sagittal plan. The *arrow* indicates the aneurysm